RESEARCH SAVING SPINDLE UNIT BEARINGS FOR LATHE MACHINES

Azamatov Shokhrukh Qoplonbek ugli Master's student at Navoi State University of Mining and Technologies

Jurayev Musurmon Avlakulovich Associate Professor, PhD at Almalyk State Technical Institute

Narzullaev Mamur Nusratillo ugli Master's student at Navoi State University of Mining and Technologies

Oripov Dostonjon Rustamjon ugli Master's student at Navoi State University of Mining and Technologies

Tilloev Olim Oybekovich Master's student at Navoi State University of Mining and Technologies

Abstract. The spindle unit is a critical component of machine tools, directly influencing performance, energy efficiency, and operational reliability. This review and analysis consolidate recent advances in spindle technology, focusing on condition monitoring, fault diagnosis, structural optimization, and energy-efficient design. Techniques such as vibration monitoring, acoustic emission, shock pulse method, and surface roughness measurement have been successfully applied for fault detection. Studies highlight innovations in motorized spindle bearing systems, lubrication strategies, preload optimization, thermal error control, and intelligent diagnostic methods. Analytical and experimental investigations, including multi-support spindle models and ultra-precision lathe designs, demonstrate enhanced structural rigidity, machining accuracy, and energy performance. Moreover, sustainable approaches integrating condition monitoring, remanufacturing, and advanced product-service systems offer potential economic and operational benefits.

The findings provide comprehensive insights for the development of high-performance, energy-efficient, and reliable spindle systems in modern machine tools.

Introduction

The authors [1] discussed endeavors to focus on the condition monitoring aspects on the machine tool element. In the present study, a critical subsystem has been identified based on the failure data analysis. Condition monitoring techniques like vibration monitoring, acoustic emission, Shock Pulse Method (SPM) and surface roughness have been successfully used for fault identification. [2] This paper provides a systematic review of recent technological advances in motorized spindles, with a focus on bearing systems, thermal characteristics, and intelligent fault diagnosis. By surveying mainstream products and relevant research, this study summarizes the current state of spindle bearing configurations, lubrication methods, preload strategies, thermal error control approaches, and diagnostic technologies. [3] This study presents the analysis of a typical machine tool spindle unit and highlights potential measures to improve its energy efficiency. The work is part of the “EnergieMSP” project, which aims to develop an energy-optimized spindle unit with a suitably adapted electric drive system. A comprehensive evaluation of the system was conducted directly on a machine tool to assess the energy consumption of pressurized air, tool change operations, and hydraulic standby losses. Additionally, frictional losses in the bearings, rotary unions, and the electrical drive train were examined separately on dedicated test benches. [4] This paper provides a systematic review of recent technological advances in motorized spindles, with a focus on bearing systems, thermal characteristics, and intelligent fault diagnosis. By surveying mainstream products and relevant research, this study summarizes the current state of spindle bearing configurations, lubrication methods, preload strategies, thermal error control approaches, and diagnostic technologies.[5] The spindle system of

computer numerical control (CNC) lathe is the principal energy consumer in the machine tool operating stage. Structural optimization design of spindles is regarded as an effective strategy for energy saving. Compared with previous optimization design methods for improving deformation, vibration and other traditional performance indicators of spindle, this paper proposes a method comprehensively considering energy consumption and traditional performance. [6] An analytical two-support spindle model was developed to evaluate structural rigidity, enabling the determination of optimal design parameters for the spindle. Stress–strain and natural frequency analyses performed in APM Structure3D confirmed the operational stability of the proposed spindle structure. [7] In this paper, a four-axis ultra-precision lathe for machining large-scale drum mould with microstructure surface is presented. Firstly, because of the large dimension and weight of drum workpiece, as well as high requirement of machining accuracy, the design guidelines and component parts of this drum lathe are introduced in detail, including control system, moving and driving components, position feedback system and so on. [8] A series of different cooling concepts have been researched and developed in recent decades. These developments have been made for different purposes. They also differ considerably in terms of their cooling principles and cooling performance. In this article, these cooling approaches and the motivations for their development are described. [9] This article describes a sustainable remanufacturing approach for in-service machine tools, integrating condition monitoring, diagnosis, and product-service systems. The proposed model restores used machines to like-new or improved performance, upgrades their functionality, and demonstrates significant economic and social benefits. [10] This article describes the behavior of spindle assemblies with different roller bearing configurations and spacings, deriving empirical formulas to predict spindle tip flexure. It highlights how these formulas can save time in spindle calculations and ensure accurate rotation and positioning of cutting tools in metal-cutting machines.

2. Methods and Experiments

[1] Experimental studies were conducted on a precision tool room lathe in a laboratory environment at the Machine Dynamics Lab, ITMMEC, Indian Institute of Technology (IIT) Delhi. The spindle was supported by a pair of pre-loaded taper roller bearings at the front end and a heavy bush bearing at the rear end. Lubrication was provided using deliberately contaminated grease prepared at the Centre for Polymer Science and Engineering, IIT Delhi, to simulate bearing wear conditions. The test bearings used were SKF taper roller bearings (size code 30209) with an inner diameter of 45 mm, outer diameter of 85 mm, width of 19 mm, and 18 rollers with a pressed steel cage.

A mild steel workpiece with a diameter of 25 mm and length of 150 mm was used, with an overhang of 80 mm to minimize vibration during cutting. Cutting conditions, tool inserts, and tool holder specifications were maintained according to standard parameters.

Accelerometers were mounted at two locations on the spindle to record vibration signals. Overall vibration levels and vibration spectra were measured using an FFT analyzer (ONO SOKKI) for all cutting conditions. Acoustic emission was captured using a hydrophone (SEH) through a jet of cooling lubricant directed to the cutting zone. Shock pulse measurements were performed on the test bearings to confirm bearing faults under contaminated lubrication. Surface roughness of the turned workpiece was measured offline using Taly-Surf 6 (Taylor Hobson). To minimize the influence of tool wear and breakage, fresh cutting tool inserts were used for each experiment.

[2] Motorized spindles were analyzed by application type (grinding, engraving/milling, drilling) and bearing support type (rolling bearings). Key technical parameters such as rotational speed, output torque, mounting diameter,

dynamic precision, and tool interface type were collected from commercial samples. This method was chosen to systematically compare spindle performance across different applications and to identify how design features affect machining efficiency and precision.

Experimental tests were conducted on rolling bearing-supported spindles, focusing on centrifugal force, vibration, and temperature rise for different bearing materials (Si_3N_4 ceramic vs. steel). These experiments were performed to evaluate bearing performance under high-speed conditions, verify their suitability for high-speed and high-precision machining, and guide the selection of optimal bearing types for motorized spindles.

The rigidity of the spindle-tooling structure was analyzed for a multi-purpose lathe (model MS03) equipped with duplexed angular contact ball bearings in a "tandem-O" preload scheme. The spindle unit, including the modular tooling, was modeled as a constant cross-section cantilever beam on two supports, with bearing compliance represented by springs of finite stiffness. This method was chosen to accurately evaluate the effect of bearing and spindle dimensions on overall structural stiffness under operational loads.

Analytical and symbolic computations were performed using the Maple environment, allowing the determination of spindle end displacement and overall compliance as a function of cantilever length, inter-support distance, and bearing stiffness. Preload effects and design constraints were included to simulate realistic operating conditions.

To optimize spindle rigidity, the ratio of spindle span (inter-support distance) to spindle diameter was analyzed. The maximum deflections and rotation angles of the cantilever were evaluated, ensuring that structural deformations remained within permissible limits for turning and boring operations.

This approach provides a systematic framework for predicting and optimizing spindle stiffness, guiding both the design of spindle-tooling assemblies and their practical implementation in multi-functional lathe operations.

An ultra-precision four-axis drum lathe was designed to machine large-scale roll workpieces with high accuracy and microstructure requirements. Key design considerations included high spindle load capacity, high rotational accuracy, low heat generation, minimal vibration, and thermal drift. The lathe has two rotary axes (C & B) and two linear axes (X & Z), with aerostatic spindles mounted in the headstock and tailstock for the C axis, and torque motors installed for rotary motion. Granite was chosen for the machine bed to ensure long-term stability and thermal resistance, while hydrostatic guideways and linear motors were used for precise and responsive linear motion.

To evaluate the static structural distortion caused by the heavy roll workpiece (up to 1000 kg), a finite element analysis (FEA) was performed using ANSYS. The drum lathe was meshed with hexahedral elements, and the deflections of the roll workpiece in vertical (Y) and horizontal (X) directions were calculated. Results showed a maximum vertical deflection of 82.3 μm, while horizontal displacement was negligible (16.9 nm), indicating the weakest rigidity link at the four-jaw chuck and transition piece.

The load characteristics of the aerostatic spindle were analyzed using computational fluid dynamics (CFD) simulations in FLUENT. A half-model of the aerostatic journal bearing was simulated under an air supply pressure of 0.5 MPa. The effects of bearing eccentricity and rotational speed on carrying capacity and stiffness were studied. The simulations showed that the spindle system could achieve a carrying capacity of 9464.5 N and stiffness of 1370.2 N/μm, sufficient to support the 1000 kg roll workpiece.

This methodology allowed for the evaluation of structural rigidity, spindle load capacity, and bearing performance, ensuring the lathe design meets strict precision and stability requirements for ultra-precision machining of large-scale drum moulds.

The development of motorized spindles was analyzed by reviewing the historical and technological evolution from the 1980s to the present. Initially, gear-driven spindles and magnetic bearings were used to achieve high speeds, but their industrial adoption was limited due to complexity and cost. Technological advances in bearing materials, lubrication, and motor drives since the mid-1990s enabled the widespread use of motorized spindles with rolling bearings, including hybrid ceramic elements.

To evaluate spindle performance, the specific speed parameter (n·dm) was used as an indicator, where n is the operating speed and dm is the mean bearing diameter. Historical trends of n·dm values and motor power density were analyzed from product catalogs of leading spindle manufacturers, complemented by market research data from 2019.

This approach was adopted to identify trends in maximum speed, torque, and power output, and to assess how improvements in bearing technologies and permanent-magnet synchronous motors (PMM) have enhanced machining efficiency. Despite these advances, the shaft-bearing system remains a key limiting factor, particularly in managing heat generation and maintaining high rotational accuracy.

In metal-cutting machines, the spindle assembly is responsible for primary rotation and precise positioning of cutting tools. The present study focuses on the 1A616 lathe with different roller bearing configurations to evaluate static and dynamic spindle characteristics under specified cutting conditions (cutting depth t = 3 mm, feed s = 0.1 mm/rev, spindle speed n ≈ 630 rpm, cutting power N = 2.01 kW).

The methodology involved calculating the spindle tip and workpiece masses, gear parameters, and rotational characteristics based on standard formulas and GOST

specifications. Cutting forces and power were determined analytically, and bearing configurations were selected according to the velocity coefficient (d–n), which considers the spindle diameter and maximum rotational speed.

Static deformation of the spindle assembly was analyzed using REGRESS software to interpolate spindle flexure along the spindle axis. Nine calculation points were evaluated, and the mean deviation from the polynomial fit was 8–10%. This approach allowed the determination of spindle tip deflection as a function of bearing spacing, providing guidance for selecting appropriate roller bearing configurations for rough machining of a 24-kg workpiece.

This methodology ensures that spindle rigidity, bearing configuration, and load distribution are optimized for accuracy, minimal deformation, and effective cutting performance.

3. Results

[1] The overall vibration levels increased with the depth of cut and feed rate in all experimental conditions. Vibration values were higher at location 2, where the spindle was supported on a bush bearing, compared to location 1, which used taper roller bearings. In bearings with defects, the vibration amplitudes were significantly higher than those recorded under defect-free conditions, and the increase became more pronounced as the size of silica contaminant particles increased. Frequency spectrum analysis revealed a residual imbalance in the spindle, with a predominant 1X component around 28 Hz. Peaks corresponding to bearing defect frequencies were clearly observed, and their amplitudes increased with the particle size of the contamination.

Acoustic emission (AE) measurements exhibited trends similar to the vibration data. For defect-free bearings, AE levels increased with increasing depth of cut and feed rate. Bearings with contamination displayed higher AE signals, and larger

contaminant particles caused more pronounced AE levels, indicating greater wear or micro-impact events within the bearing contact zones.

Surface roughness of the machined workpiece also increased with depth of cut and feed rate, under both healthy and faulty bearing conditions. The presence of defective bearings led to a higher rate of increase in surface roughness, particularly at larger feed rates and deeper cuts. The influence of larger contamination particles appeared more on surface waviness than on micro-roughness, which aligned with the observed increase in vibration levels.

Flame atomic absorption spectrometry (FAAS) analysis of the bearing grease revealed that the atomic iron content increased under contaminated conditions compared to defect-free conditions. Interestingly, as the size of silica contaminant particles increased, the iron content showed a slight decrease, suggesting that smaller particles may contribute more to abrasive wear of the bearing components.

The APM Shaft module does not account for the angular compliance of the spindle unit, which significantly influences the deformation characteristics of the designed structure. Therefore, to obtain more accurate results in modeling and stress–strain analysis, the APM Structure3D module was used. This module enables three-dimensional complex analysis while incorporating the angular flexibility of the spindle supports.

During the modeling process, a skeleton representation of the spindle was constructed, where bar elements were defined between nodes corresponding to changes in loading or stiffness. Each bar element had defined geometric parameters and was connected to adjacent elements through these nodes. The spindle assembly was divided into several sections that reflected real structural features such as splines, keyways, grooves, chamfers, and fillets. The module allowed the use of

arbitrary and multiply connected cross-sections, and a parametric spline section model was added to the section library for use in the spindle structure.

The loading conditions for the spindle were formed from multiple force components acting with different magnitudes and directions. For this purpose, the APM Structure-3D “Loading” toolkit was used, enabling the placement of these force components into an abstract load space within the spindle model. The supports were defined using a combination of rigid and elastic fixations, each acting independently along specific coordinate directions at the designated nodes. Rigid restraints were applied by restricting displacements and rotations along the X and Y axes.

Stress analysis in the APM Structure3D environment showed the distribution of stresses during a typical turning operation on the multipurpose machine MS03. According to the color scale of the results, the equivalent stress values (SVM), calculated using the energy theory of strength, remained below the allowable yield stress of the spindle material (DIN 20Cr4 steel, $[\tau] = 635$ MPa), even with the yield factor $k\tau = 2$.

The module also provided an evaluation of the dynamic characteristics of the spindle system, including natural frequencies and corresponding vibration modes. The software computed 16 natural frequencies with an accuracy of 0.01%. The third and fourth vibration modes, which reflect the deformation shapes of the spindle at their respective frequencies, were also obtained and analyzed.

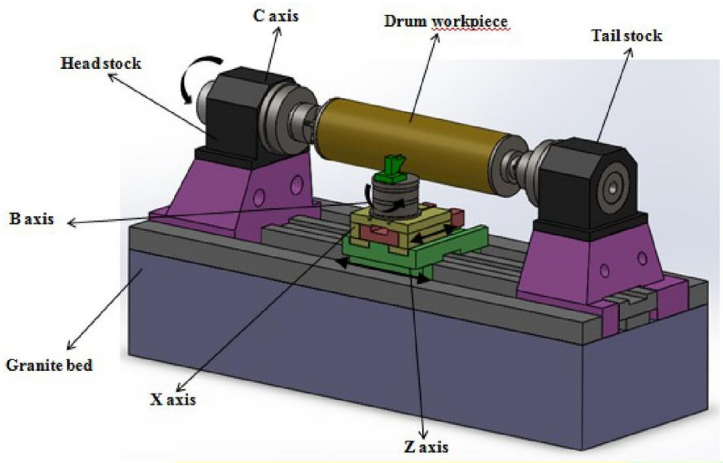


Figure 1: Structural layout of four-axis ultra-precision drum lathe

The structural and functional performance of the four-axis ultra-precision roll lathe was evaluated through static deformation analysis and aerostatic spindle load-capacity simulations. Due to the extremely heavy roll workpiece (up to 1000 kg), the lathe structure was designed symmetrically to minimize deformation. ANSYS-based static analysis revealed that the primary deflection occurred in the vertical (Y) direction, with a maximum displacement of approximately 82.3 μm, mainly concentrated in the four-jaw chuck and transition sections, which represent the weakest rigidity link. In contrast, the horizontal deflection (X direction) was negligible, equivalent to a positional change of only 16.9 nm, indicating that lateral structural distortion has almost no influence on cutting accuracy.

Table 1:

Specifications of four-axis ultra precision drum lathe

Terms	Specification
C axis	Max. speed
Resolution	0.036 arcsec
Z axis	Max. speed
Resolution	5nm
Stroke	1500mm
X axis	Max. speed
Resolution	5nm
Stroke	240mm
B axis	Max. speed
Resolution	0.13 arcsec
Rotation error	≤0.05 μm
Drum mould	Max. weight
Max. length	1400mm

Max. diameter	**400mm**

The aerostatic spindle system, which must support high loads while maintaining ultra-high rotational precision, was analyzed using CFD simulations in FLUENT. A half-model of the journal bearing was used due to structural symmetry. Results showed clear pressure differentiation between the upper and lower regions of the air film caused by eccentricity, which generates the load-bearing capability. At an air-supply pressure of 0.5 MPa, the spindle achieved a maximum carrying capacity of 9464.5 N and a stiffness of 1370.2 N/μm. Considering that two aerostatic spindles are installed—one in the headstock and one in the tailstock, the system provides sufficient support for roll workpieces up to 1000 kg, fully meeting the load requirements of ultra-precision machining.

The combined results demonstrate that the lathe's symmetric structural configuration, natural-granite bed, hydrostatic guideways, and high-stiffness aerostatic spindle system effectively suppress static deformation and maintain machining precision. As a result, the machine satisfies the stringent accuracy, load-capacity, and stability requirements necessary for ultra-precision drum mould fabrication.

[9] The remanufacturing of in-service machine tools demonstrates significant improvements in performance, resource utilization, and operational efficiency. For the TCA125 heavy-duty horizontal lathe, the remanufacturing process restored the machine to a like-new condition, with geometric accuracy, positional accuracy, thermal behavior, speed characteristics, and noise levels all meeting original factory standards. Additionally, the integration of advanced mechanical and electrical components enhanced the functional capabilities of the machine, increasing productivity by 10–20% and reducing fault-response time by approximately 30%. These performance benefits were achieved while keeping remanufacturing costs at

only 20–30% of the price of a new machine, extending service life and increasing economic value for users.

Table 3 Precision of redesigned and remanufactured TCA125 × 800 heavy-duty horizontal lathe

From: In-service machine tool remanufacturing: a sustainable resource-saving and high-valued recovery approach

Criteria		Standards	Test value
Radial run-out on the axis of the spindle conical hole	Near the end of the spindle	0.015	0.010
	500 mm from the end face of the spindle	0.040	0.038
Parallelism of the spindle axis to the Z-axis	In the horizontal plane (Z-X)	0.030 in 500	0.018
	In the vertical plane (Z-Y)	0.040 in 500	0.016
Radial runout of the spindle tip		0.020	0.008
Radial runout of the tailstock		0.020	0.018
Equal height between the main axis and the tailstock axis		0.060	0.056
Bidirectional positioning accuracy *A*	X-axis	0.025	0.0199
One-way repeat positioning accuracy *R*	X-axis	0.008	0.0079
One-way repeat positioning accuracy *R*	X-axis	0.008	0.0078
Reverse difference *B*	X-axis	0.010	0.0098
	Z-axis	0.031	0.0279

Resource-related outcomes also proved substantial. More than 80% of the machine's total mass—including major components such as the headstock, tailstock, bed, base, and carriage—was successfully reused, reducing the need for new materials and lowering environmental impact. The remanufactured TCA125 lathe demonstrated energy savings exceeding 20% due to upgraded servo drives, spindle systems, hydraulic units, lubrication systems, and CNC controls. Enhanced intelligence and monitoring capabilities further supported efficient energy management.

Improvements in machining accuracy reduced material waste, while upgraded feed systems, travel ranges, spindle speed, and supporting technologies facilitated a 20–40% increase in both resource and energy efficiency. Overall, the remanufacturing of the TCA125 lathe confirmed that in-service machine tool remanufacturing is an effective high-value strategy for extending equipment life, reducing production **costs, improving performance, and conserving critical resources across the machine's life cycle.**

[10] For the spindle used in rough machining of a 24-kg workpiece, three bearing configurations of normal accuracy were analyzed, since the use of high-precision bearings in such conditions would be impractical. The REGRESS software was employed to process the deformation data of spindle assembly No. 1 with a bearing spacing of 200 mm. The software enables the selection of a suitable analytical function to fit the calculated points, displays the relative deviations from the fitted curve, and provides interpolation capability.

Based on the introduced deformation data, REGRESS generated an empirical polynomial for spindle flexure, expressed as:

$$y = 0.780401446242224 - 0.0138091817650x + 9.31363091609494 \times 10^{-5}x^2 - 4.3458374916416 \times 10^{-5}x^3 + 1.19314993377104 \times 10^{-9}x^4 - 1.2557182965058 \times 10^{-12}x^5.$$

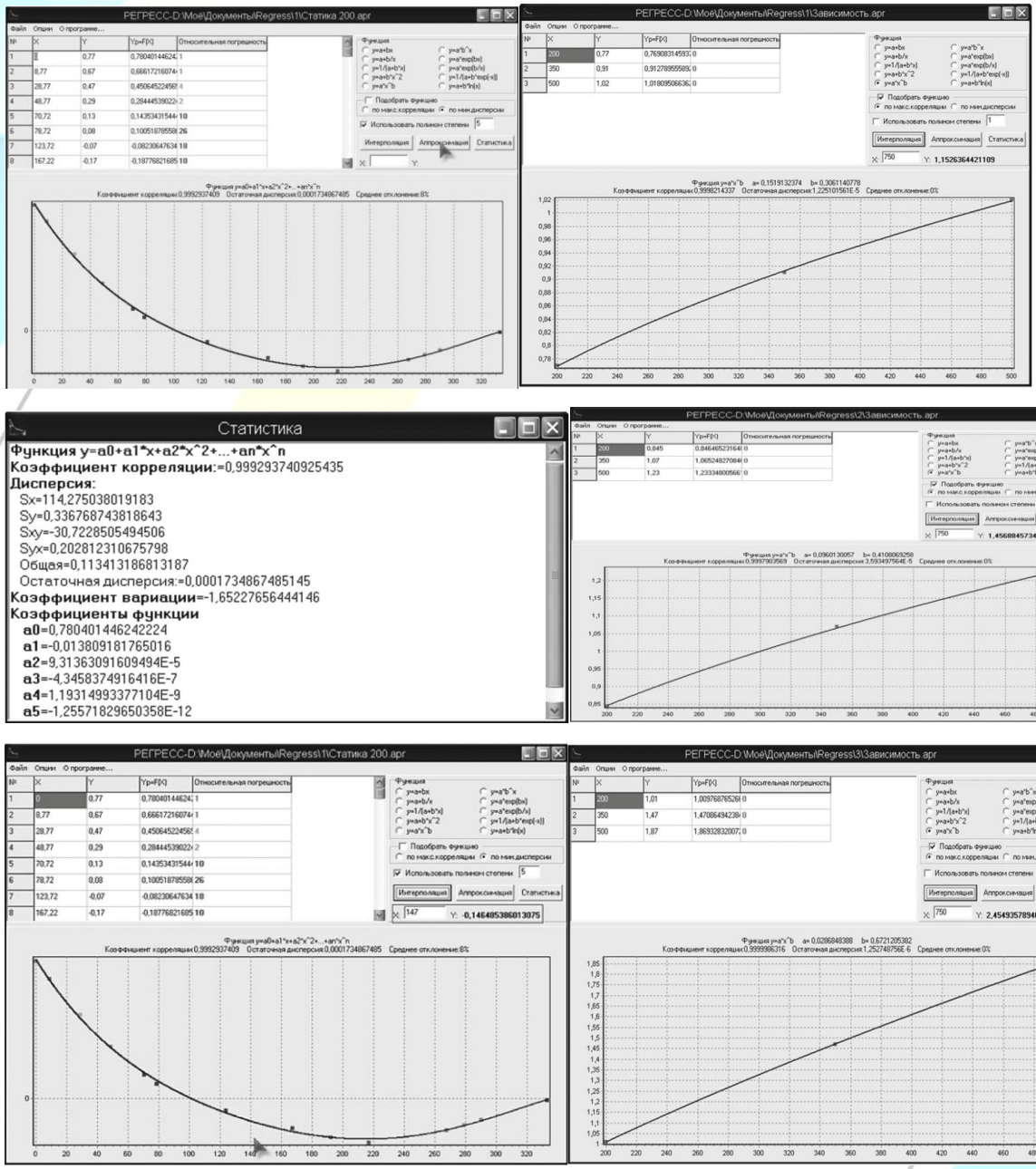
Interpolation using this model allows the determination of spindle deflection at any position along the X-axis, and the average deviation between calculated and fitted values remains within 8–10%.

Further analysis focused on determining the relationship between bearing spacing and spindle tip deflection. For the first bearing configuration, REGRESS produced the empirical equation:

$$y = 0.1519x^{0.3061},$$

from which the spindle flexure at a spacing of 750 mm was found to be 1.1526 μm. For bearing configurations 2 and 3, the corresponding empirical models were:

$$y = 0.096x^{0.4108}, y = 0.0286x^{0.672}.$$



These formulas allow rapid prediction of spindle deflection for different bearing arrangements and spacing values. The use of REGRESS significantly reduces computation time, lowering design costs for new spindle assemblies. The established empirical models for various configurations demonstrate the potential for developing an automated reference handbook covering a wide range of spindle diameters and bearing layouts.

4. Conclusion

This study comprehensively examined spindle unit behavior in lathe machines through vibration analysis, acoustic emission monitoring, surface integrity evaluation, structural modeling, and spindle-load simulations. Experimental investigations demonstrated that increasing cutting parameters led to higher vibration and acoustic emission levels, with defective and contaminated bearings causing significantly amplified responses. Frequency analysis confirmed the presence of residual spindle imbalance and revealed distinct bearing-defect frequencies, whose amplitudes intensified with larger contaminant particles. Correspondingly, surface roughness measurements showed notable degradation under faulty bearing conditions, especially at higher feeds and depths of cut.

FAAS results indicated elevated iron content in contaminated grease samples, confirming increased wear within the bearing system. Structural analysis using APM Structure3D showed that the spindle stresses remained below allowable limits, while modal analysis provided natural frequencies and vibration modes essential for predicting dynamic behavior. For ultra-precision lathe applications, finite element simulations revealed that heavy roll workpieces primarily induce vertical deformation, with negligible horizontal displacement. Aerostatic spindle CFD simulations confirmed sufficient load capacity and stiffness to support up to 1000 kg workpieces.

Overall, the combined experimental and analytical findings highlight the critical role of bearing health, spindle structural rigidity, and high-stiffness aerostatic supports in achieving stable operation, maintaining machining accuracy, and ensuring long-term reliability of lathe spindle systems.

5. References

[1] Saravanan, S., Yadava, G.S. & Rao, P.V. Condition monitoring studies on spindle bearing of a lathe. *Int J Adv Manuf Technol* **28**, 993–1005 (2006). https://doi.org/10.1007/s00170-004-2449-0

[2] Xie, P., Zhang, Z., Liao, H. *et al.* Industrial motorized spindle systems: challenges and trends in bearing, thermal, and fault diagnosis. *Int J Adv Manuf Technol* (2025). https://doi.org/10.1007/s00170-025-16905-w

[3] Abele, E., Sielaff, T., Schiffler, A., Rothenbücher, S. (2011). Analyzing Energy Consumption of Machine Tool Spindle Units and Identification of Potential for Improvements of Efficiency. In: Hesselbach, J., Herrmann, C. (eds) Glocalized Solutions for Sustainability in Manufacturing. Springer, Berlin, Heidelberg. https://doi.org/10.1007/978-3-642-19692-8-49

[4] Xie, P., Zhang, Z., Liao, H. *et al.* Industrial motorized spindle systems: challenges and trends in bearing, thermal, and fault diagnosis. *Int J Adv Manuf Technol* (2025). https://doi.org/10.1007/s00170-025-16905-w

[5] Y. Lv, C. Li, Y. Tang, X. Chen and X. Zhao, "Towards Lightweight Spindle of CNC Lathe Using Structural Optimization Design for Energy Saving," *2020 IEEE 16th International Conference on Automation Science and Engineering (CASE)*, Hong Kong, China, 2020, pp. 220-225, doi: 10.1109/CASE48305.2020.9216976.

[6] Krol, O., Sokolov, V. (2021). Research of the Spindle Units for Multioperational Lathes in the APM WinMachine Environment. In: Ivanov, V., Trojanowska, J., Pavlenko, I., Zajac, J., Peraković, D. (eds) Advances in Design, Simulation and Manufacturing IV. DSMIE 2021. Lecture Notes in Mechanical Engineering. Springer, Cham. https://doi.org/10.1007/978-3-030-77719-7_5

[7] Proceedings Volume 9283, 7th International Symposium on Advanced Optical Manufacturing and Testing Technologies: Design, Manufacturing, and Testing of Micro- and Nano-Optical Devices and Systems; 92830I (2014) https://doi.org/10.1117/12.2070005

[8] Denkena, B., Bergmann, B. & Klemme, H. Cooling of motor spindles—a review. *Int J Adv Manuf Technol* **110**, 3273–3294 (2020). https://doi.org/10.1007/s00170-020-06069-0

[9] Du, Y., He, G., Li, B. *et al.* In-service machine tool remanufacturing: a sustainable resource-saving and high-valued recovery approach. *Environ Dev Sustain* **24**, 1335–1358 (2022). https://doi.org/10.1007/s10668-021-01499-6

[10] Mitin, E.V., Sul'din, S.P. Static and Dynamic Spindle Characteristics in Lathes with Different Roller Bearing Configurations. *Russ. Engin. Res.* **43**, 577–580 (2023). https://doi.org/10.3103/S1068798X23050271